

## OECD/NEA BENCHMARK CALCULATIONS FOR ACCELERATOR DRIVEN SYSTEMS

**M. Cometto**

CEA/PSI

5232 Villigen, Switzerland

**B.C. Na**

OECD/NEA

Le Seine Saint-Germain, 12, blvd des Iles, 92130 Issy-les-Moulineaux, France

**P. Wydler**

5452 Oberrohrdorf, Switzerland

### Abstract

In order to evaluate the performances of the codes and the nuclear data, the Nuclear Science Committee of the OECD/NEA organised in July 1999 a benchmark exercise on a lead-bismuth cooled sub-critical system driven by a beam of 1 GeV protons. The benchmark model is based on the ALMR reference design and is optimised to burn minor actinides using a “double strata” fuel cycle strategy. Seven organisations (ANL, CIEMAT, KAERI, JAERI, PSI/CEA, RIT and SCK•CEN) have contributed to this exercise using different basic data libraries (ENDF/B-VI, JEF-2.2 and JENDL-3.2) and various reactor calculation methods. Significant discrepancies are observed in important neutronic parameters, such as  $k_{\text{eff}}$ , reactivity swing with burn-up and neutron flux distributions.

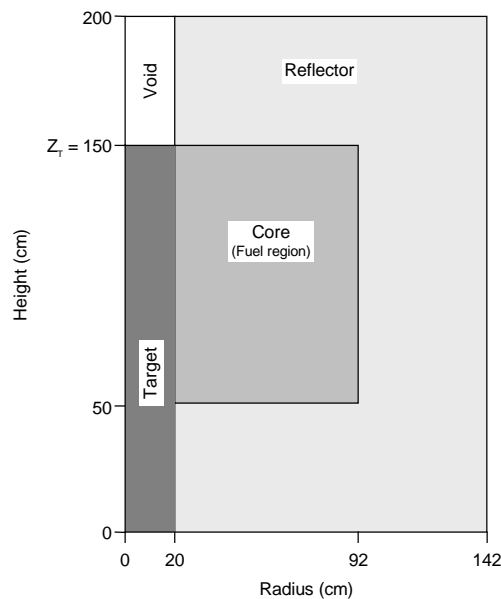
## 1. Introduction and benchmark specification

Recognising a need for code and data validation in the area of accelerator driven systems (ADS), the OECD/NEA Nuclear Science Committee organised in 1994 a benchmark on a sodium cooled sub-critical system with a tungsten target and minor actinide (MA) and plutonium nitride fuel [1]. In that benchmark, considerable differences in calculated initial  $k_{\text{eff}}$  and burn-up reactivity swing indicated a need for refining the benchmark specification and continuing the exercise with a wider participation [2,3]. The present benchmark was therefore launched in July 1999 to resolve the discrepancies observed in the previous exercise and to check the performances of reactor codes and nuclear data for ADS with unconventional fuel and coolant. The choice of lead-bismuth as a coolant and target material reflects the increased interest in this technology.

The ADS is designed to operate as a MA burner in a “double strata” strategy, featuring a fully closed fuel cycle with a top-up of pure MA. Two fuel compositions are prescribed in accordance with this strategy. In the start-up core, MAs are mixed with plutonium from UOX-fuelled LWRs. In the equilibrium core, the fuel represents an asymptotic composition reached after an indefinite number of cycles. Both fuel compositions differ strongly from the usual U-Pu mixed oxide (MOX) composition. The fuel is diluted with zirconium as an inert matrix for the core to give a  $k_{\text{eff}}$  of about 0.95 at BOL. Since the emphasis is on code and data validation in the energy region below 20 MeV, a predefined spallation neutron source, produced with HETC assuming a proton energy of 1 GeV and a beam radius of 10 cm, was provided to the participants.

The R-Z benchmark model, shown in Figure 1, comprises four regions: a central lead-bismuth target zone, a void zone in the beam duct region, a multiplying region which consists of homogenised fuel, cladding and lead-bismuth coolant and, finally, an outer reflector zone. The reactor operates at a nominal power of 377 MW<sub>th</sub> and the core has a residence time of 5 years. To simulate a load factor of 0.85, the power is reduced to 320 MW<sub>th</sub> in the burn-up calculations. At EOL the fuel reaches an average burn-up of approximately 200 GWd/t<sub>HM</sub>.

Figure 1. R-Z model of ADS



The choice of adopting the ALMR reference system as a basis for the benchmark model has the advantage that a detailed plant concept is available and the characteristics of the plant with normal cores has already been analysed in great detail, including transient and beyond design basis behaviour. The present benchmark model is therefore also suited for transient benchmarks.

As a follow-up to the present benchmark, a transient benchmark dealing with the beam trip problem of the ADS is currently being defined. Preliminary results of the current benchmark exercise were presented in November 1999 at the OECD/NEA Workshop on Utilisation and Reliability of High Power Accelerators in Aix-en-Provence [4].

## 2. Results and discussion

Seven institutions participated in the benchmark, using nuclear data mainly from ENDF/B-VI, JEF-2.2 and JENDL-3.2. For the core analysis, both deterministic and Monte Carlo methods were applied. The list of participants, basic libraries and codes used are summarised in Table 1.

Table 1. List of participants, basic data libraries and codes

Organisation	Basic library	Codes used	Method
<b>ANL</b> (USA)	ENDF/B-VI ENDF/B-V for lumped FP	MC <sup>2</sup> -2, TWODANT, REBUS-3	Deterministic
<b>CIEMAT</b> (Spain)	JENDL-3.2 ENDF/B-VI for fission yields	EVOLCODE system (NJOY, MCNP-4B, ORIGEN-2.1)	Monte Carlo
<b>KAERI</b> (Korea)	JEF-2.2 JENDL-3.2 for Pb and <sup>242m</sup> Am	TRANSX-2.15, TWODANT, DIF3D-7.0, REBUS-3	Deterministic
<b>JAERI</b> (Japan)	JENDL-3.2	ATRAS (SCALE, TWODANT, BURNER, ORIGEN-2)	Deterministic
<b>PSI/CEA</b> (CH/France)	ERALIB I (JEF-2.2 based)	ERANOS, ORIHET	Deterministic
<b>RIT</b> (Sweden)	JEF-2.2	NJOY, MCNP-4B, MCB, ORIGEN-2	Monte Carlo
<b>SCK•CEN</b> (Belgium)	JEF-2.2 ENDF/B-VI for Pb and <sup>233</sup> U	NJOY97.95, MCNP-4B, ORIGEN-2	Monte Carlo

In addition to their reference solution, some participants provided additional results obtained with different methods or basic libraries. In particular, RIT provided neutron flux distributions for the equilibrium core obtained with ENDF data and  $k_{\text{eff}}$  results for the start-up core based on the JENDL library.

In the following, we summarise the most important results of the benchmark exercise. In particular, we focus on the one-group microscopic cross-sections, the neutron spectrum, the neutron flux distributions, the integral parameters  $k_{\text{inf}}$  and  $k_{\text{eff}}$  as well as the  $k_{\text{eff}}$  variation with the burn-up. Other important parameters such as the external neutron source strength and safety parameters are also discussed.

In the analysis of the results, it is necessary to consider how the participants accounted for the nuclear power in the system. Whereas ANL, CIEMAT, KAERI and PSI/CEA took into account the energy coming from both fissions and captures, JAERI and SCK•CEN considered only the energy coming from fissions and RIT neglected both the energy coming from captures and from delayed

neutrons. Since the neutron flux is normalised to the given reactor power of 377 MW, neglecting the contribution of some reactions to the power leads to an overestimation of the flux. The effect can be estimated to be about 4% for JAERI and SCK•CEN and about 9% for RIT; it therefore has an important influence, especially on the fuel burn-up and on the neutron flux distributions.

The main neutronic characteristics reported by the participants are summarised in Tables 2 and 3. Table 2 refers to the start-up core and Table 3 refers to the equilibrium core.

Table 2. Main neutronic characteristics of the start-up core

Parameters	Organisation						
	<i>ANL</i>	<i>CIEMAT</i>	<i>JAERI</i>	<i>KAERI</i>	<i>PSI/CEA</i>	<i>RIT</i>	<i>SCK•CEN</i>
Library	ENDF	JENDL	JENDL	JEFF	JEFF	JEFF	JEFF
$k_{inf}$	1.15894	1.13732	1.15920	1.13256	1.13141	1.149	1.14729
$k_{eff}$ at BOL	0.98554	0.9570	0.9650	0.94546	0.94795	0.9590	0.9590
P/A ratio *	1.307	1.245	1.253	1.226	1.228	1.220	1.241
Source (n/s)-BOL	6.1E17	1.65E18	1.25E18	4.11E18	2.26E18	2.54E18	2.29E18
Source (n/s)-EOL	4.12E18	3.51E18	2.88E18	7.33E18	3.96E18	4.83E18	4.54E18
Neutron's median energy (keV)	210	212	162	222	214	220	220
Coolant void reactivity (pcm) **	3 161 2 433	3 905 3 214	3 813 3 048	3 686 2 596	2 870 1 655	2 904 1 863	2 896 1 681
Fuel Doppler effect (pcm) ***	0 13	38.2 323.7	20.2 31.9	16.5 27.2	6.2 12.4	48 53	11 48.7
$\beta_{eff}$ at BOL (pcm)	156	246	173.5	–	184.0	195	–

Table 3. Main neutronic characteristics of the equilibrium core

Parameters	Organisation						
	<i>ANL</i>	<i>CIEMAT</i>	<i>JAERI</i>	<i>KAERI</i>	<i>PSI/CEA</i>	<i>RIT</i>	<i>SCK•CEN</i>
Library	ENDF	JENDL	JENDL	JEFF	JEFF	JEFF	JEFF
$k_{inf}$	1.14420	1.11629	1.14192	1.13366	1.13165	1.150	1.14884
$k_{eff}$ at BOL	0.96895	0.9370	0.9494	0.94174	0.94374	0.9570	0.95509
P/A ratio *	1.308	1.241	1.258	1.258	1.260	1.245	1.274
Source (n/s)-BOL	1.39E18	2.54E18	1.94E18	4.49E18	2.55E18	2.70E18	2.47E18
Source (n/s)-EOL	3.18E18	2.38E18	2.00E18	5.80E18	2.86E18	3.39E18	2.64E18
Neutron's median energy (keV)	185	188	152	181	179	188	183
Coolant void reactivity (pcm) **	3 318 2 154	4 511 2 582	4 138 2 821	3 902 2 034	2 732 1 925	3 045 1 605	3 144 1 681
Fuel Doppler effect (pcm) ***	20 12	17.1 277.6	30.4 45.8	23.0 43.7	4.2 5.8	45 49	98 103
$\beta_{eff}$ at BOL (pcm)	116	221	145.2	–	155.9	188	–

\* Ratio between production and absorption reaction rates in the heavy metals.

\*\* Calculated as  $k_{eff}^{voided} - k_{eff}^{ref}$  for the BOL (first row) and EOL (second row).

\*\*\* Calculated as  $(k_{eff}^{980K} - k_{eff}^{1580K}) / (k_{eff}^{980K} \cdot k_{eff}^{1580K})$  for the BOL (first row) and EOL (second row).

## 2.1 One-group microscopic cross-sections and $k_{inf}$

The one-group microscopic cross-sections provided by ANL, KAERI, PSI/CEA and SCK•CEN are obtained by means of a cell calculation; i.e. the fundamental mode neutron spectrum of the fuel cell is used for averaging the cross-sections. CIEMAT, JAERI and RIT derived one-group microscopic cross-sections from a reactor calculation; the latter cross-sections represent averages over the core fuel zone and, therefore, differ from those obtained from cell calculations. As shown by additional calculations made by PSI/CEA and SCK•CEN, the differences due to the averaging method are between 4.5% and 13% for the one-group capture cross-sections and less than 6% for the one-group fission cross-sections.

The figures at the end of this section show microscopic one-group capture cross-sections of the most relevant isotopes in the equilibrium core. Figure 2 compares cell averaged and Figure 3 compares core averaged one-group cross-sections.

The cross-sections show some correlation with the basic data used: the JENDL-based cross-sections are in good agreement for all the isotopes. Some discrepancies appear between the JEFF-based cross-sections: when comparing the core averaged data, RIT and SCK•CEN give very close results which, however, differ from the PSI/CEA results for the majority of isotopes. When comparing the cell averaged data, the results provided by KAERI, PSI/CEA and SCK•CEN generally differ from one another.

A direct comparison of both cell- and core-averaged cross-sections requires caution. Nevertheless, the following general conclusions can be made: when comparing one-group cross-sections, based on different basic libraries, good agreement can be observed only for uranium isotopes (not presented in the figures). Large discrepancies are observed for plutonium isotopes, particularly for the capture cross-sections. Compared to other libraries, ENDF gives a higher value for  $^{238}\text{Pu}$  and lower values for the other isotopes. The values obtained with JEFF and JENDL are closer, except for the isotopes 238 and 241.

Considerable discrepancies between cross-sections based on different libraries are observed also for neptunium, americium and curium. For example, JENDL gives by far the highest capture cross-sections for  $^{243}\text{Cm}$ ,  $^{246}\text{Cm}$  and  $^{247}\text{Cm}$ , and ENDF gives significantly lower fission cross-sections for  $^{242}\text{Cm}$ ,  $^{243}\text{Cm}$  and  $^{245}\text{Cm}$  (not presented in this paper).

The  $k_{inf}$  results (presented in Tables 2 and 3) show quite a spread. The maximum differences are 2.5% for the start-up core and 3.0% for the equilibrium core. Interestingly, no clear correlation with the nuclear data used can be observed. Significant discrepancies are observed between the two JENDL-based results (about 2.0%). The four JEFF-based results can be grouped into two classes, characterised by high (RIT and SCK•CEN) and low (KAERI and PSI/CEA) values. Another interesting effect is that JEFF predicts similar  $k_{inf}$  values for both cores, whereas ENDF and JENDL predict a  $k_{inf}$  difference of about 1.5% between the start-up and the equilibrium cores.

Figure 2. Microscopic capture cross-sections for the equilibrium core (cell averaged)

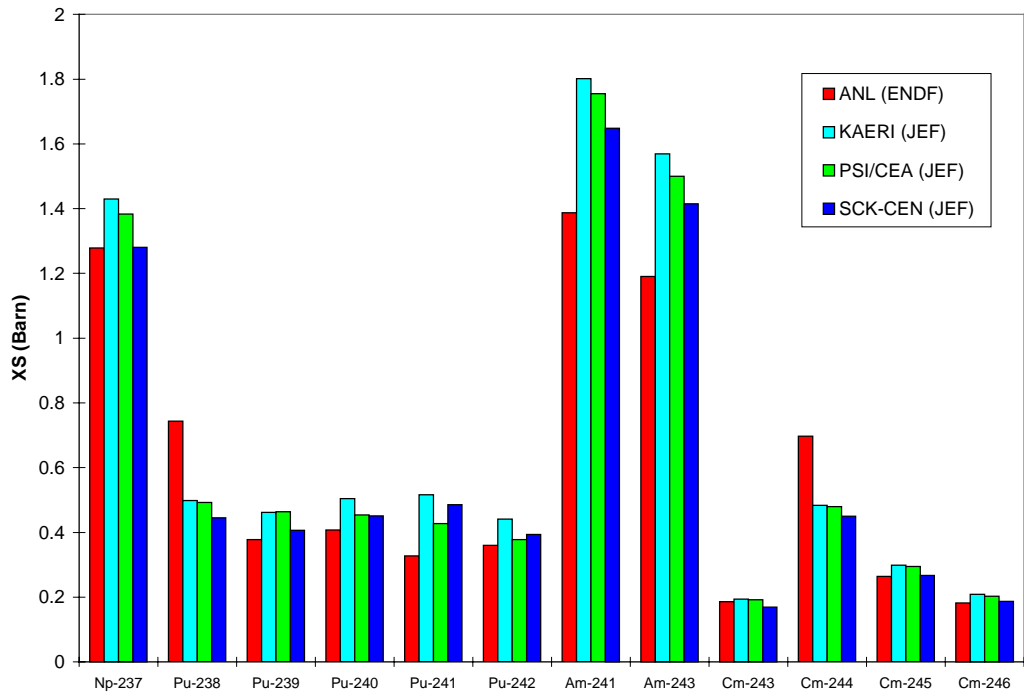
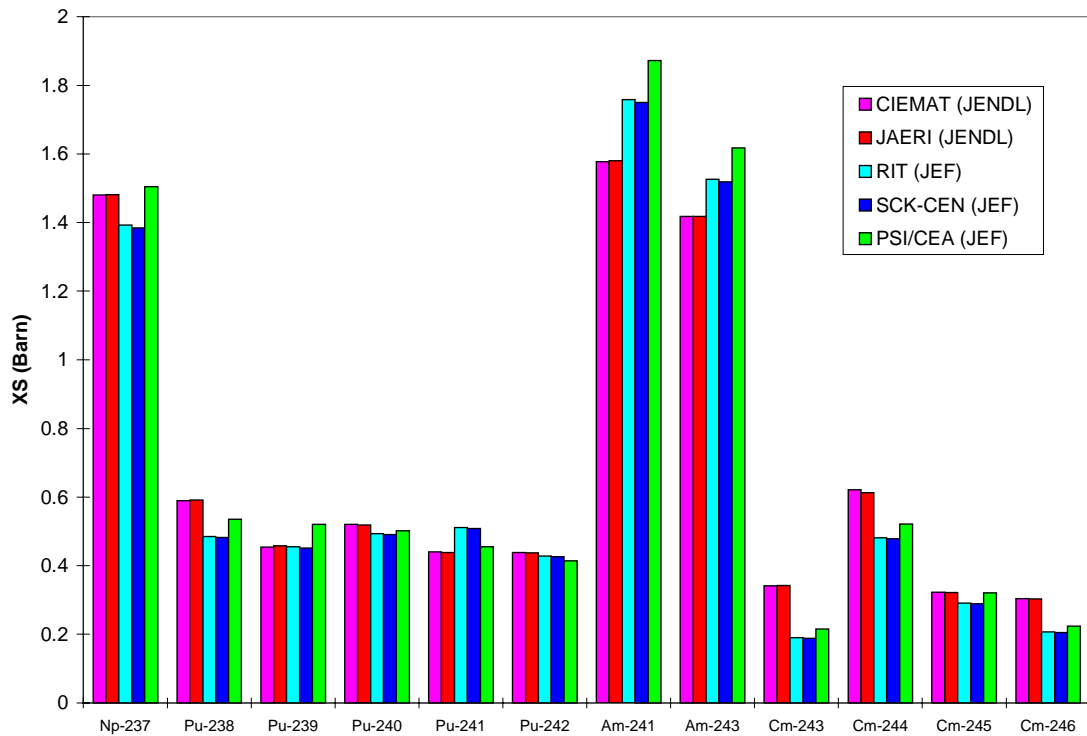


Figure 3. Microscopic capture cross-sections for the equilibrium core (core averaged)



## 2.2 $k_{\text{eff}}$ at beginning of life and $k_{\text{eff}}$ variation

The  $k_{\text{eff}}$  values at beginning of life (see Tables 2 and 3) show a maximum discrepancy of 4% for the start-up core; the spread in the  $k_{\text{eff}}$  values is slightly reduced for the equilibrium core. The  $k_{\text{eff}}$  values do not show a clear correlation with the library used, indicating that the sensitivity of the results to the data processing route and/or the neutron transport approximation also has to be investigated. 1% of the discrepancies arise from the two ENDF-based calculations and 0.8% from the three JENDL-based results. The four JEFF-based results can be grouped into two classes characterised by high (RIT and SCK•CEN) and low (KAERI and PSI/CEA)  $k_{\text{eff}}$  values. However, comparing these results is difficult because only RIT used the complete JEF-2.2 library. PSI/CEA used the library ERALIB1 (adjusted from JEF-2.2) and KAERI and SCK•CEN used data for Pb from JENDL and ENDF respectively.

A systematic sensitivity analysis performed by KAERI using a simplified 1-D model of the start-up core enables us to estimate the impact of the nuclear data on  $k_{\text{eff}}$  [5]. The results show that the  $k_{\text{eff}}$  values are lower by 2 250 pcm for JEF and by 1 160 pcm for JENDL, when all the important actinides are substituted from the reference ENDF-based calculation. Overall, the  $k_{\text{eff}}$  obtained using JEFF is 2 070 pcm lower than the reference ENDF-based result; the differences arise mainly from heavy metals (-2 250 pcm), lead (+680 pcm) and  $^{15}\text{N}$  (-420 pcm) while the contribution of bismuth is small (-73 pcm). JENDL also gives a lower  $k_{\text{eff}}$  value (-2800 pcm) mainly due to the contribution of lead (-1 100 pcm) and heavy metals (-1 160 pcm). The contribution of  $^{15}\text{N}$  and bismuth (-450 and -77 pcm) is similar to that for JEFF.

From the reaction rates provided by the participants, the production over absorption (P/A) ratio is calculated for all the heavy nuclides and it is presented in Tables 2 and 3. ANL (ENDF) predicts by far the highest values for both core configurations, whereas the other results are closely grouped. The two JENDL-based results are similar and, for the four JEFF-based results, SCK•CEN gives the highest value and RIT the lowest value for both core compositions. The ratios of production to absorption are similar for the start-up and the equilibrium cores when using ENDF and JENDL data. However, all four JEFF-based results give larger values (+2.5%) for the equilibrium core than for the start-up core. Interestingly, the  $k_{\text{eff}}$  values are not correlated in a systematic way with P/A ratios as one would expect. In particular, all four JEFF-based solutions give a lower P/A ratio but a higher  $k_{\text{eff}}$  in the start-up core. ANL, CIEMAT and JAERI calculated similar P/A values but different multiplication factors for both cores.

The multiplication factors for the two cores do not exhibit consistent biases. This may be due to the fact that the two cores are not dominated by the same producers and absorbers. From the submitted reaction rate balance components, it can be deduced that the production rate is dominated by  $^{239}\text{Pu}$ ,  $^{241}\text{Am}$  and  $^{241}\text{Pu}$  in the start-up core and by  $^{238}\text{Pu}$  and  $^{245}\text{Cm}$  in the equilibrium core. The absorption rate is dominated by  $^{241}\text{Am}$ ,  $^{239}\text{Pu}$  and  $^{243}\text{Am}$  in the start-up core and by  $^{243}\text{Am}$  and  $^{238}\text{Pu}$  in the equilibrium core.

The  $k_{\text{eff}}$  variations with burn-up are shown in Figures 4 and 5 and the respective burn-up reactivity drops,  $k_{\text{BOC}}-k_{\text{EOC}}$ , including decomposition of the global reactivity drop into actinide and fission product components, are given in Tables 4 and 5. In addition to the solution obtained with the JEFF library, RIT presented, for the start-up core, an additional solution obtained with JENDL data.

Figure 4.  $k_{\text{eff}}$  variation in the start-up core

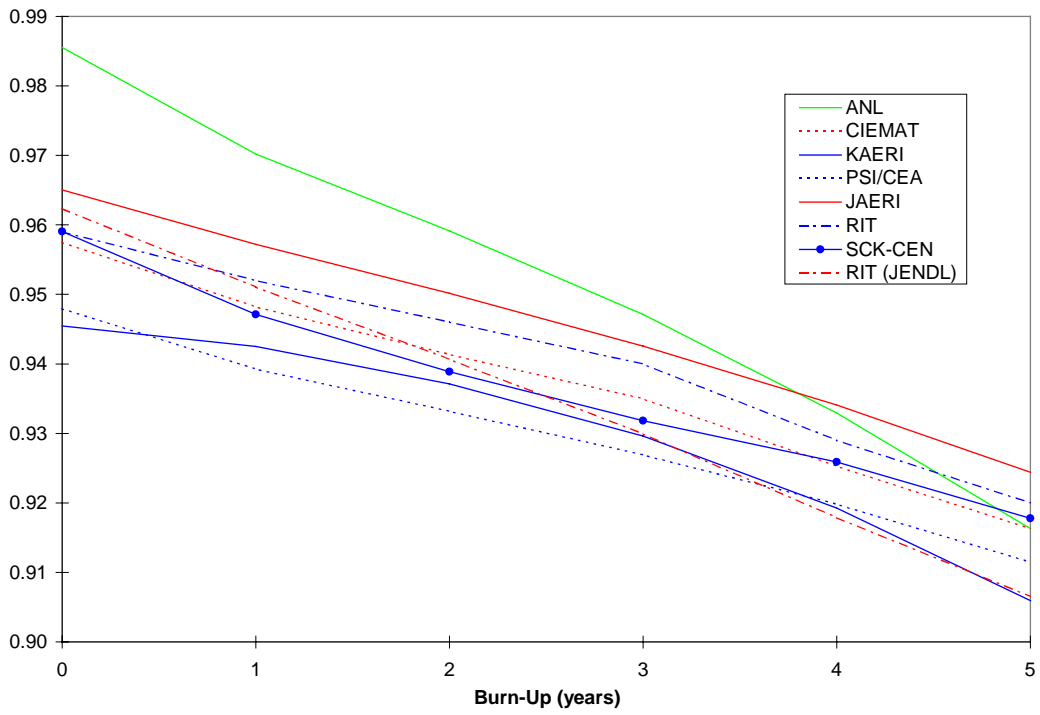
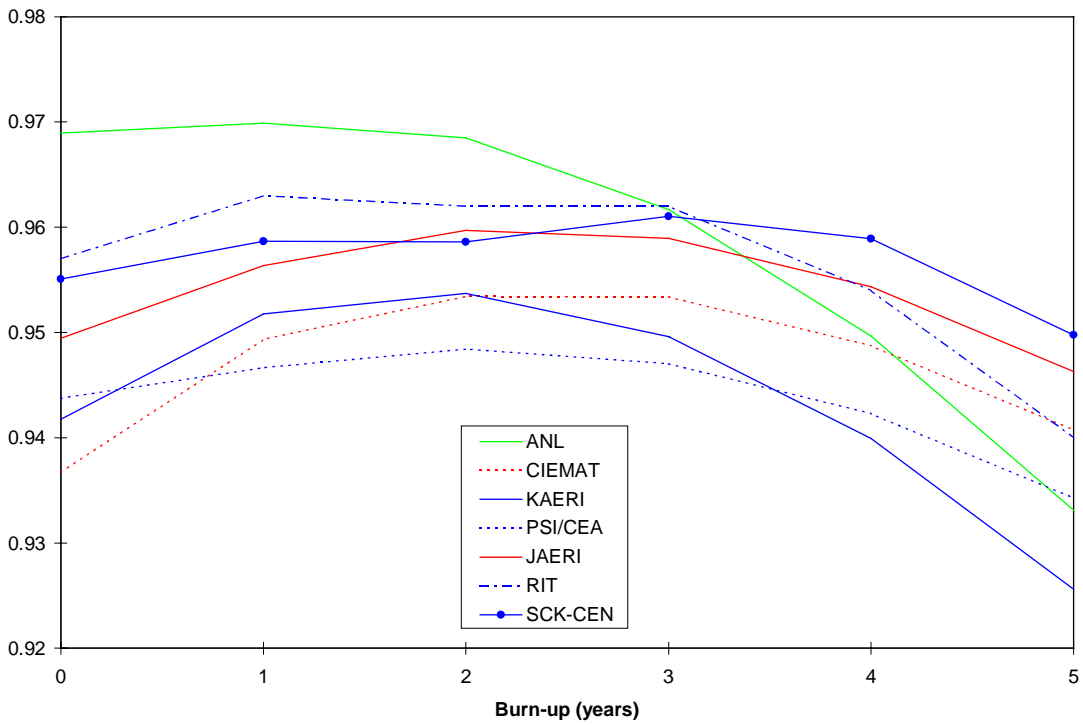


Figure 5.  $k_{\text{eff}}$  variation in the equilibrium core



The burn-up reactivity drop values,  $k_{\text{BOC}} - k_{\text{EOC}}$ , range from 0.036 to 0.069 in the start-up core and from -0.004 to 0.036 in the equilibrium core. ANL (ENDF) predicts, in both cases, by far the highest reactivity drop. The total reactivity drop values in the start-up core are close for five participants (CIEMAT, KAERI, JAERI, JEFF-based RIT and SCK•CEN) with values between 3 900 and 4 100 pcm but this result hides compensating effects between fission products and heavy metals contributions and is fortuitous. The results are more spread for the equilibrium core.

Neither the actinide nor the fission product components are well correlated with the nuclear data library used. Only the contribution of the actinides gives similar results for three of the four JEFF-based results. Other possible causes of discrepancies can be related to the treatment of fission products. In particular, it is questionable whether lumped fission products generated for U and Pu can be representative for a system where a significant fraction of the fissions arise from minor actinides with a higher mass number, such as Am and Cm. However no obvious correlation can be observed related to the use of individual or lumped fission products.

Table 4. Start-up core: end of cycle reactivity drop components (in units of  $10^3 \Delta k$ )

$\Delta k$ from	ENDF	JENDL			JEFF			
	<i>ANL</i>	<i>CIEMAT</i>	<i>JAERI</i>	<i>RIT</i>	<i>KAERI</i>	<i>PSI/CEA</i>	<i>RIT</i>	<i>SCK•CEN</i>
Actinides	28	28	14	22	3	8	4	16
FP's	41	13	27	34	37	28	35	25
Total	69	41	41	56	40	36	39	41

Table 5. Equilibrium core: end of cycle reactivity drop components (in units of  $10^3 \cdot k$ )

$\Delta k$ from	ENDF	JENDL		JEFF			
	<i>ANL</i>	<i>CIEMAT</i>	<i>JAERI</i>	<i>KAERI</i>	<i>PSI/CEA</i>	<i>RIT</i>	<i>SCK•CEN</i>
Actinides	-11	-18	-27	-27	-26	-27	-17
FP's	45	14	30	43	35	44	22
Total	36	-4	3	16	9	17	5

### 2.3 Neutron spectrum

Neutron spectra are calculated for both cores at  $R = 56$  cm and  $Z = 100$  cm; this point corresponds to the centre of the fuel region where the neutron spectrum is dominated by the fission neutrons. From the submitted neutron spectra, median energies were calculated (see Tables 1 and 2).

Good agreement is observed for most of the participants except for JAERI, which predicts a clearly softer spectrum (its median energy is about 20% lower than the others). The spectra provided by the other six participants show a good agreement especially for the energy range above 5-10 keV that covers approximately 95% of the neutrons. It is only in the lower resonance region (between 100 eV and 1 keV) that the differences between the results become pronounced. Finally, it is interesting to notice that the spectrum in the equilibrium core is softer than that in the start-up core.

## 2.4 Neutron flux distribution

One radial flux distribution corresponding to the mid-plane and two axial flux distributions corresponding, respectively, to the centre of the target and the fuel zone were requested. Considerable differences between the participants are observed, especially for the radial neutron flux distribution and for the axial flux distribution in the target zone. In particular, ENDF-based results (ANL and RIT) estimate by far the lowest neutron flux through the target. The discrepancies are also significant in the fuel region, where differences in flux level and in peak flux position appear. These discrepancies can be partially explained by the different level of sub-criticality: a system with a lower  $k_{\text{eff}}$  needs more external neutrons in order to maintain the chain reaction. This results in a more peaked axial flux in the target, at the interface with the duct, and a displacement of the axial flux peak in the fuel towards the upper part of the core.

An additional study was performed with ERANOS in order to assess the impact of the  $k_{\text{eff}}$  value on the neutron flux distribution. By modifying appropriately the  $\nu$  values for reproducing the  $k_{\text{eff}}$  values submitted by the participants, neutron flux distributions were recalculated for each participant. From these distributions, spatial dependent correction factors were obtained. Finally, the neutron flux distributions supplied by the participants were rescaled for the reference  $k_{\text{eff}}$  value of 0.95 using these spatial dependent correction factors. The rescaled neutron flux distributions are presented in Figures 6, 7 and 8 and refer to the equilibrium core.

Figure 6. Axial flux distribution in the target region; results scaled to a  $k_{\text{eff}}$  value of 0.95

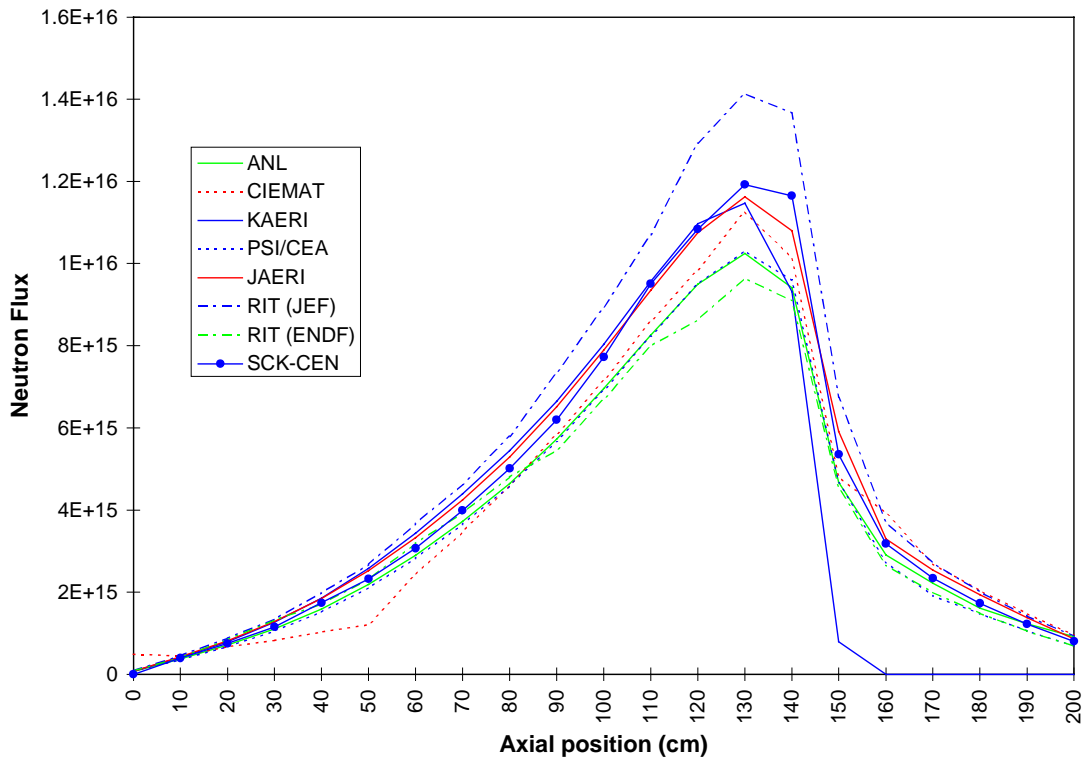


Figure 7. Axial flux distribution in the fuel region; results scaled to a  $k_{eff}$  value of 0.95

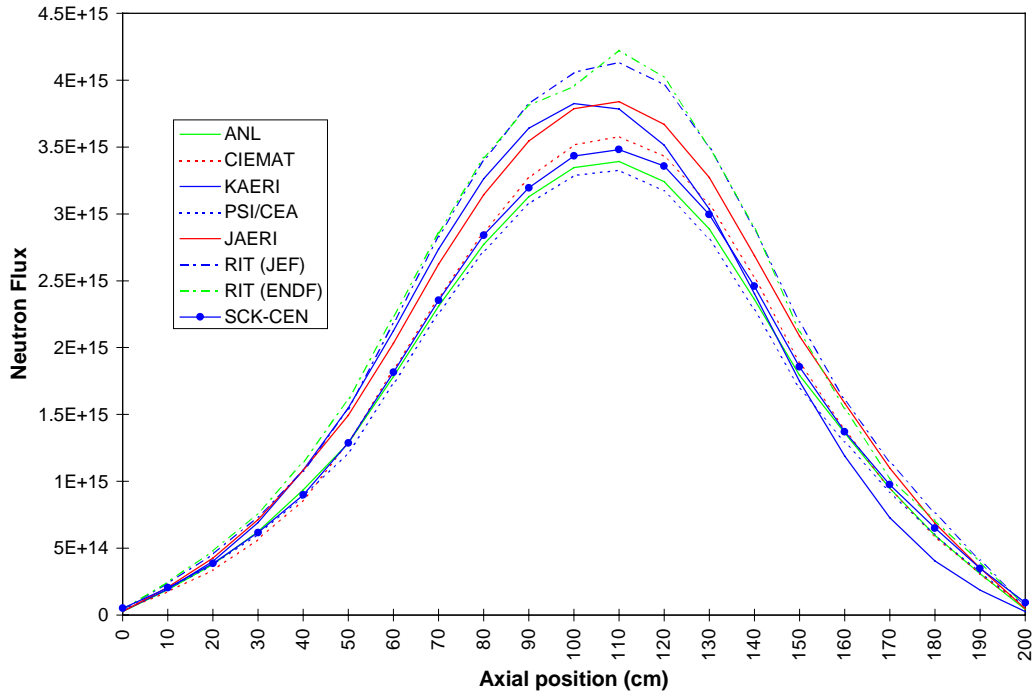
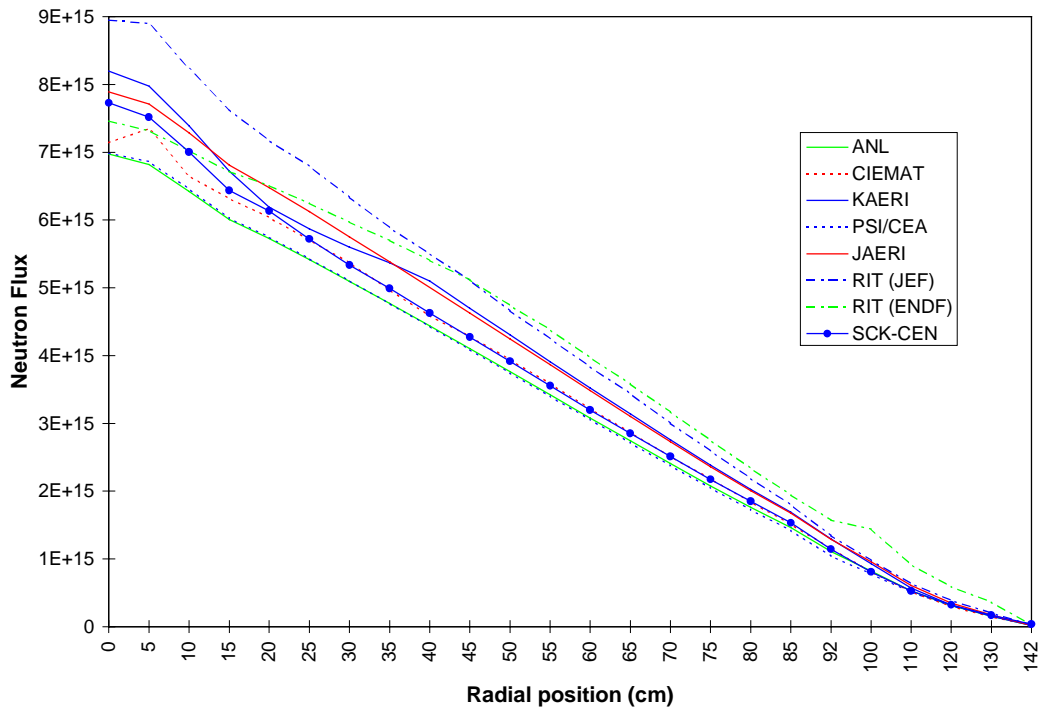


Figure 8. Radial flux distribution in the mid-plane; results scaled to a  $k_{eff}$  value of 0.95



In the fuel region, the shape of the axial neutron flux distributions is in good agreement for most participants. However, the peak position reported by KAERI is shifted to the core centre ( $Z = 100$  cm). The spread in the absolute value of the flux is still significant and the difference

between the highest and the lowest value (obtained by RIT and PSI/CEA respectively) is about 20%. As expected, the discrepancies in the axial neutron distributions in the target region become considerably smaller after the adjustment. The shapes of the flux distributions have a similar trend and the values are less spread. Similar considerations apply to the radial neutron flux distributions corresponding to the mid-plane. Referring to the normalisation of flux to power mentioned earlier, the neutron flux values provided by RIT, SCK•CEN and JAERI are overestimated with respect to the other participants and should be reduced correspondingly (9% for RIT, 4% for JAERI and SCK•CEN).

Even with the adjustment taking into account the  $k_{\text{eff}}$  effect, there still remain differences in the flux distributions, especially in the absolute value of the flux and its shape. Large discrepancies are observed in the shape of the axial flux in the target calculated by CIEMAT and KAERI. The CIEMAT result shows a distinct feature in the lowest part of the target region, due to the geometry model used: the lowest part of the target (the first 50 cm) was replaced by a void region. The KAERI result has a vanishing flux in the void zone; that is probably due to the diffusion approximation.

## 2.5 Source strength

The source strength, i.e. the number of neutrons per second that the ADS needs in order to maintain the chain reaction, is an important parameter because it is directly proportional to the required accelerator power. Its value is given by the following equation [6]:

$$N = \frac{P_{\text{th}} \cdot v_k}{E_f} \cdot \left( \frac{1}{k} - 1 \right) \cdot \frac{1}{\phi^*}$$

where  $N$  is the number of neutrons/s,  $P_{\text{th}}$  the thermal power,  $v_k$  and  $E_f$ , respectively, the average number of neutrons and the average energy released per fission in the fuel,  $k$  the multiplication factor of the system without source and  $\phi^*$  the importance of spallation neutrons relative to fission neutrons.

The results, presented in Tables 2 and 3, for the beginning and for the end of irradiation, show quite a spread: at BOL, the ratio between the highest (KAERI) and the lowest (ANL) values is about 7 for the start-up core and 3 for the equilibrium core. The other three JEFF-based results lie in a similar range (maximum difference of about 10%) and the two JENDL-based results show a difference of about 30% for both core configurations.

As the above equation indicates, the required number of external neutrons is strongly dependent on the multiplication factor. It may be interesting to isolate that effect by dividing the source strength value by  $(1/k-1)$  in order to remove the differences due to the multiplication factor (at least partially, knowing that  $\phi^*$  is also dependent on  $k$ ). The numerical value obtained in that way is dependent on  $P_{\text{th}}$ ,  $v_k$ ,  $E_f$  and  $\phi^*$  and therefore should be close for all the participants. The values obtained are quite discrepant, KAERI presenting by far the highest value. Interestingly, the correlation between the three other JEFF-based results turns out to be fortuitous; RIT and SCK•CEN results are closer and the PSI/CEA value is similar to that obtained by ANL. The two JENDL-based results lie in a similar range.

## 2.6 Isotopic composition at end of irradiation

From the submitted results (not shown in this paper), significant discrepancies in the isotopic

composition at the end of irradiation are observed. The results seem only partially correlated with the nuclear data libraries used.

Before analysing the isotopic composition of the irradiated fuel, it is interesting to calculate the fraction of heavy metals that fissioned after five years of irradiation. Surprisingly, the values are strongly different and can be grouped into two classes characterised by a high “burn-up” (KAERI, RIT and SCK•CEN, all using the JEFF library) and a low “burn-up”. The former values are between 21.3% and 22% and the latter between 18.5% and 18.8%. The discrepancy in the total number of heavy metals at EOL is therefore considerable (more than 15%) and is not fully understood.

As for the isotopic compositions at the end of irradiation, a clear dependence on the “burn-up” is observed. In comparison with the other participants, RIT, JAERI and SCK•CEN (high burn-up) report lower values for burned-up isotopes during the irradiation, such as  $^{237}\text{Np}$ ,  $^{241}\text{Am}$  and  $^{243}\text{Am}$  and higher values for build-up isotopes (in the start-up core only), such as  $^{238}\text{Pu}$ ,  $^{242}\text{Cm}$  and  $^{244}\text{Cm}$ .

The discrepancies are important not only for the minor actinides such as  $^{237}\text{Np}$ ,  $^{241}\text{Am}$  and  $^{243}\text{Am}$  (up to 10% relative to the average) but also for the Pu isotopes. Large differences are observed especially for  $^{238}\text{Pu}$ ,  $^{240}\text{Pu}$  and  $^{241}\text{Pu}$  where the results of SCK•CEN strongly deviate from the others.

Some discrepancies in the results are also related to differences in the branching ratios or to different treatment of some reactions. For example, the differences observed in the  $^{242}\text{Cm}$  and  $^{242\text{m}}\text{Am}$  concentrations are due to discrepancies in the branching ratios used for the  $(n,\gamma)$  reaction of  $^{241}\text{Am}$ . Most participants used the 0.2/0.8 values, whereas RIT used 0.225/0.775, PSI/CEA 0.15/0.85 and SCK•CEN 0.09/0.91. Consequently RIT gives the highest and PSI/CEA and SCK•CEN the lowest concentration of  $^{242\text{m}}\text{Am}$ . As expected, an opposite effect is observed on the  $^{242}\text{Cm}$ . Discrepancies are observed in the concentrations of  $^{236}\text{U}$  and  $^{235}\text{U}$  in the KAERI and SCK•CEN results. In the start-up core, very low concentrations of these isotopes are reported, whereas in the equilibrium core their results are in acceptable agreement with the other participants. This probably indicates a different treatment of the  $(n, 2n)$  reaction for  $^{237}\text{Np}$ , which should be thoroughly investigated.

## 2.7 Safety parameters

Coolant void reactivity calculations are traditionally difficult. Only integral values for the coolant void reactivity from  $k_{\text{eff}}$  difference calculations are available. The JENDL-based calculations by CIEMAT and JAERI give similar results (agreement within about 10%). Assuming that the Monte Carlo calculations by CIEMAT and RIT can be considered as reference calculations which are only sensitive to differences in nuclear data, the decrease in the BOL coolant void reactivity arising from the substitution of JENDL by JEFF is about 30% (26% for the start-up core and 32% for the equilibrium core). For the other JEFF-based coolant void reactivity predictions, one observes a maximum deviation of 30% with respect to the RIT prediction. It is interesting to notice that, in the ANL and JAERI case, the voided core becomes supercritical.

A general observation on the calculated Doppler reactivity is that it represents an almost “zero effect” on the system. Knowing that the magnitude of the Doppler reactivity in fast spectrum systems was demonstrated with an uncertainty of  $\pm 15\%$ , it is difficult to make a comparison of these small values dispersed around zero. Nevertheless, since the Doppler reactivity comes essentially from capture reactions in the thermal energy region, a more thorough insight into the calculation procedures used by the participants, especially energy self-shielding treatment in their calculations, would be necessary to understand the origin of discrepancies among them.

The isotope specific  $\beta_{\text{eff}}$  values calculated from the two libraries (ENDF/B-VI and JEF-2.2) are in good agreement. However, ANL (ENDF/B-VI) gives a total  $\beta_{\text{eff}}$  value smaller than that of JAERI because the contributions of  $^{242\text{m}}\text{Am}$ ,  $^{243}\text{Am}$  and Cm isotopes were not taken into account (the delayed neutron data for these isotopes are not available in ENDF/B-VI used by ANL). JAERI used the delayed neutron data of  $^{242\text{m}}\text{Am}$ ,  $^{243}\text{Am}$  and  $^{245}\text{Cm}$  isotopes from JENDL-3.2. PSI/CEA took into account the contribution of all the isotopes; its results therefore give the largest value among the results from ANL, JAERI and PSI/CEA. The Monte Carlo calculations give larger  $\beta_{\text{eff}}$  values. RIT used the delayed neutron data based on ENDF/B-VI, but did not consider  $^{242\text{m}}\text{Am}$ ,  $^{243}\text{Am}$  and Cm isotopes, whereas CIEMAT used the delayed neutron data based on JENDL-3.2 in its calculations. In general, it is seen that the results of the  $\beta_{\text{eff}}$  calculations depend on the accuracy of the delayed neutron data used.

### 3. Conclusions

Seven organisations contributed to this benchmark exercise using different basic data libraries and reactor analysis codes and applying both deterministic and Monte Carlo methods. The analysis of the results shows significant discrepancies in important neutronic parameters, such as  $k_{\text{inf}}$ ,  $k_{\text{eff}}$  and burn-up reactivity swing. Strong discrepancies appear also in the estimation of the external neutron source, i.e. a parameter which determines the requested accelerator power.

As demonstrated by a separate parametric study, the impact of the different basic nuclear data on these integral parameters is important but it is not sufficient to fully explain the discrepancies observed in the results. In future benchmark exercises which may be based on an experimental result, attention should therefore be given to both the data processing route and the neutron transport approximations. Concerning the burn-up calculations, attention should be given to the treatment of the fission products and to the actinide decay chains noting that in minor actinide burner cores different isotopes are involved compared to MOX-fuelled cores.

#### *Acknowledgements*

The authors express their gratitude to all the participants who devoted their time and effort to this benchmark exercise.

## REFERENCES

- [1] OECD/NEA NSC Task Force on Physics Aspects of Different Transmutation Concepts, *JAERI Proposal of Benchmark Problem on Method and Data to Calculate the Nuclear Characteristics in Accelerator-based Transmutation System with Fast Neutron Flux*, NEA/NSC/DOC(1996), 10 April 1996.
- [2] H. Takano *et al.*, *Benchmark Problems on Transmutation Calculation by the OECD/NEA Task Force on Physics Aspects of Different Transmutation Concepts*, Proc. Int. Conf. on the Physics of Nuclear Science and Technology, 5-8 October 1998, Long Island, USA, 1462.
- [3] *Calculations of Different Transmutation Concepts: An International Benchmark Exercise*, OECD/NEA report, NEA/NSC/DOC(2000)6, February 2000.
- [4] B.C. Na, P. Wydler and H. Takano, *OECD/NEA Comparison Calculations for an Accelerator-driven Minor Actinide Burner: Analysis of Preliminary Results*, NEA-NSC Workshop on Utilisation and Reliability of High Power Accelerators, 22-24 November 1999, Aix-en-Provence, France, (To be published).
- [5] J.D. Kim and C.S. Gil, KAERI, Private Communication.
- [6] H. Takahashi and H. Rief, *Concepts of Accelerator Based Transmutation Systems*, Proc. of the Specialists' Meeting on Accelerator-based Transmutation, 24-26 March 1992, PSI Villigen, Switzerland, 2-26.

